processes

MDPI

Article

Distributed Secondary Control of Islanded Microgrids for Fast Convergence Considering Arbitrary Sampling

Yinqiu Hong [1], Jihua Xie [1,*] and Fang Fang [2]

[1] School of Electrical Engineering, Southeast University, Nanjing 210096, China; 220192780@seu.edu.cn
[2] Electric Power Research Institute of State Grid Zhejiang Electric Power Co., Ltd., Hangzhou 310000, China; fang_ne@163.com
* Correspondence: jihua.xie@seu.edu.cn

Abstract: This paper proposes a novel distributed secondary control of MGs for fast convergence considering asynchronous sampling. With the employment of the algorithm, optimal power sharing and voltage restoration are implemented simultaneously. First, the hierarchical control objectives concerned with economic operation and voltage quality are introduced. Then, the execution process of the fast convergence algorithm is described for weighted average state estimation, with the illustration of corresponding features and the application in cooperative control. Further, the relevant stability issue is discussed based on large-signal dynamic modeling and a sufficient stability condition is derived based on the Lyapunov–Krasovskii theory. Our approach offers superior reliability, flexibility and robustness because of the loose implementation in terms of its performance concern, which is essential when the distributed consensus protocol is likely to yield toward deviation or even instability under arbitrary sampling and delays. The effectiveness of the proposed methodology is verified via simulations.

Keywords: arbitrary sampling; fast convergence; Lyapunov function; microgrid; secondary control

check for updates

Citation: Hong, Y.; Xie, J.; Fang, F. Distributed Secondary Control of Islanded Microgrids for Fast Convergence Considering Arbitrary Sampling. *Processes* **2021**, *9*, 971. https://doi.org/10.3390/pr9060971

Academic Editor: Achim Kienle

Received: 3 May 2021
Accepted: 21 May 2021
Published: 29 May 2021

Publisher's Note: MDPI stays neutral with regard to jurisdictional claims in published maps and institutional affiliations.

Copyright: © 2021 by the authors. Licensee MDPI, Basel, Switzerland. This article is an open access article distributed under the terms and conditions of the Creative Commons Attribution (CC BY) license (https://creativecommons.org/licenses/by/4.0/).

1. Introduction

With the increasing penetration of renewable energy resources, MGs have been manifested as a promising integration of DGs, storages and loads within identifiable electrical boundaries [1–3]. The appealing advantage of MG is that it can enter islanding mode in case of spontaneous events, which facilities uninterrupted power supplies [4,5]. Endowed with the superiorities of low complexity and high efficiency, the DC microgrid has a promising future for extensive application, where a hierarchical control structure with droop control installed in the primary control layer is commonly employed to ensure the stable and efficient operation [6–8]. However, voltage deviations and inappropriate current sharing caused by distinct output impedance are generally unavoidable in droop control.

Therefore, secondary control with the objective of system coordination is introduced to compensate for the drawbacks in primary control. The centralized architecture was adopted as an implementation pattern for cooperative control, where the collection and calculation of global information is implemented utilizing a MGCC. However, the requirement of a complex communication network reduces its reliability [9,10]. Inspired by the cooperative multi-agent technology, distributed secondary control has gained increasing popularity, where each DG receives information from its neighbors via a sparse communication network [11]. The consensus protocol provides an effective approach for distributed cooperative control based on the estimation and elimination of the disagreement across the system, and has become a mainstream algorithm in current research [12–16]. Inspired by the robust and optimal control theory, a new distributed control architecture was proposed in [14], where cooperative control objectives can be realized in the presence of system uncertainties. Based on the feedback linearization and Artstein transformation methods, a novel distributed finite-time control scheme which is resilient to communication failures

was proposed in [15]. With the assistance of a voltage sensitivity matrix in distributed control, the power sharing performance was greatly improved, and transient states were eliminated [16].

Essentially, the effectiveness of consensus-based cooperative control heavily depends on the timely and accurate acquisition of both local and neighboring information, and the update and sampling actions of individual DGs are assumed to be synchronous in most of the existing literature. However, due to the absence of a global clock, the control action of each DG will be triggered according to their local clocks, which would be diverse. Hence, neighboring information from the current control instant could be unavailable and the update action of each DG will be conducted based on the information received from the latest sampling instants of their neighboring nodes. In this premise, asynchronization manifested as sampling time offset occured [17–19], and this asynchronous issue would lead to persistent information disorder, which in turn brings about convergence deviation in consensus-based control on account of the erroneous estimation of the disagreement value and could even lead to system divergency with the expansion of deviation [20–24]. The impact of this unfavorable factor mentioned above has been investigated in [17–22]; however, to the best of knowledge, this research addressed the stability issue based on imposing restrictions on the upper bounds of sampling intervals and the approach to alleviate the adverse consequences caused by asynchronous sampling is lacking research.

Motivated by the research gap mentioned above, this paper focuses on providing an effective secondary control method to optimize the system performance in asynchronous communication scenarios. The fast convergence algorithm is first applied in MG cooperative control to implement the combination of secondary and tertiary control with a better convergence performance. Further, the sufficient condition for the algorithm stability is derived based on the Lyapunov function. The main contributions are listed below:

(1) The objectives of optimal load sharing and voltage restoration can be achieved simultaneously with a fast convergence rate due to indirect information acquisition from nodes that are multiple hops away and the exclusion of repetitive information. Further, the relevant stability issue is discussed.
(2) Compared with the consensus algorithm, the proposed algorithm shows a superior robustness in cases of asynchronous execution.
(3) The optimal load sharing criteria is derived based on simplifying the problem into a constrained extremum search of the objective function utilizing the Lagrange multiplier method.

The reminder of this paper is organized as follows: Section 2 introduces the hierarchical control and formulates the asynchronous problems. A novel secondary control scheme is proposed in Section 3 with stability analysis elaborated in Section 4. Simulations are provided in Section 5; conclusions are drawn in Section 6.

2. Problem Formulation

2.1. Control Objective

The hierarchical control structure for DC MG is presented in Figure 1, which is equipped with two hierarchies to implement different control objectives.

Generally, droop control is utilized to generate the reference for the voltage and current loops, which is formulated as

$$V_i = V_{refi} - \gamma_i i_i, \tag{1}$$

where i_i can be measured using a low-pass filter with a cut-off frequency ω_c:

$$\dot{i}_i = -\omega_c i_i + \omega_c i_{oi}, \tag{2}$$

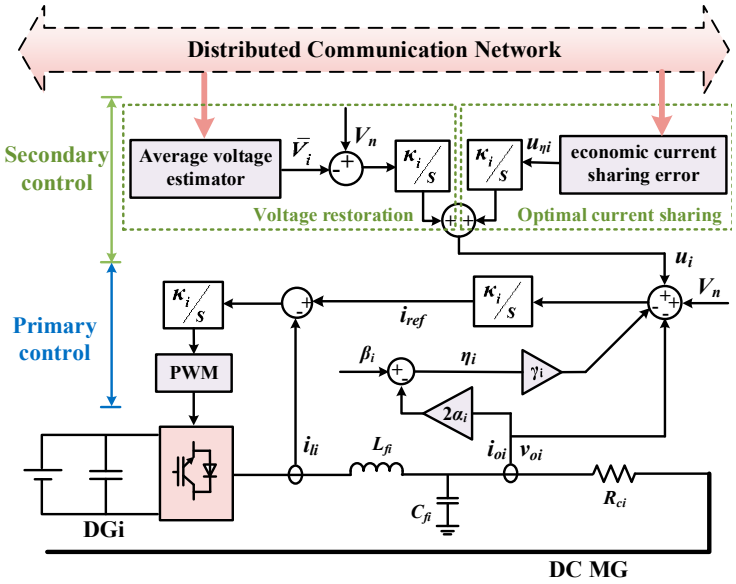

Figure 1. Hierarchical control structure.

On account of the diverse output resistances, the current sharing under droop control would be unsatisfactory. Generally, the desired allocation criteria for output currents can be expressed as $\gamma_1 i_1 = \gamma_2 i_2 = \ldots = \gamma_n i_n$, i.e., DGs are supposed to share the load currents inversely proportional to the droop coefficient. However, taking the economic issue as a primary consideration, the optimal load sharing criteria is derived and applied in this paper. The typical cost function of each distributed generation can be modeled as

$$C_i(i_i) = \alpha_i i_i^2 + \beta_i i_i + \rho_i, \tag{3}$$

Further, a constrained optimization problem can be formulated as an objective function: $\min C(i_i) = \sum_{i=1}^{n} C_i(i_i)$ with a network constraint on supply and demand balance: $\sum_{i=1}^{n} i_i = \sum_{i=1}^{nl} i_{Li} = i_D$. The Lagrange multiplier method simplifies the aforementioned problem to the extremum search of the following Lagrange function by virtue of introducing a multiplier η:

$$L = \sum_{i=1}^{n} C_i(i_i) + \eta(i_D - \sum_{i=1}^{n} i_i), \tag{4}$$

Employing the first-order derivative approach, the equation follows that

$$\frac{\partial L}{\partial i_i} = 2\alpha_i i_i + \beta_i - \eta_i = 0, \tag{5}$$

Accordingly, the incremental cost can be defined as $\eta_i(i_i) = 2\alpha_i i_i + \beta_i$ and the economic optimization condition (6) yields from (5):

$$\eta_1(i_1) = \eta_2(i_2) = \cdots = \eta_n(i_n), \tag{6}$$

i.e., the optimal operation can be achieved when the incremental costs of all DGs are equal [25].

Considering the instinct tradeoff between power sharing and individual voltage restoration, the average voltage across MG is expected to be regulated to the reference so that all voltages can be maintained within an acceptable range; hence, an observer is required for average voltage estimation without knowledge of global information.

$$\overline{V}_i = V_i + k_{i3} \int \sum_{j=1, j \neq i}^{n} a_{ij}(\overline{V}_j - \overline{V}_i), \tag{7}$$

The secondary control selects input u_i such that $\eta_i \to \eta_j$, and $\overline{V}_i \to V_{ref}$ to guarantee economic superiority and voltage restoration simultaneously.

2.2. Inconsistent Information Exchange in Consensus-Based Cooperative Control

For the sake of implementation, a discrete form of secondary control scheme is formulated as

$$\begin{aligned} V_i(k) &= V_{refi}(k) - \gamma_i i_i(k) + u_i(k) \\ u_{\eta i}(k) &= k_{i1} T_i \sum_{j=1, j\neq i}^{n} a_{ij}[\eta_j(k) - \eta_i(k)] \\ u_i(k+1) - u_i(k) &= u_{\eta i}(k) + k_{i2} T_i [V_{ref} - \overline{V}_i(k)], \end{aligned} \tag{8}$$

where $a_{ij} = 1$ suggests DGi receives information from DGj, otherwise $a_{ij} = 0$; the associated Laplace matrix L can be defined as $L = \Delta - \Lambda$, where $\Delta = \mathrm{diag}(\Delta_{ii})$ with $\Delta_{ii} = \sum_{j \in Ni} a_{ii}$ and $\Lambda = [a_{ij}]$.

The accuracy of the consensus-based control introduced above is greatly dependent on the synchronicity of information interaction. However, as depicted in Figure 2, inherent asynchronization is inevitable in the practical execution of distributed self-triggered systems given the absence of a centralized synchronization clock and independent control pattern of each DG, which is manifested as

$$\begin{aligned} \dot{x}_i(k) &= \varepsilon T_i \sum_{\rho=1, \rho\neq i}^{n} a_{\rho i}[x_\rho(k - \lambda_{ij}) - x_i(k)] \\ \dot{x}_j(k) &= \varepsilon T_j \sum_{\rho=1, \rho\neq j}^{n} a_{\rho j}[x_\rho(k - \lambda_{ij}) - x_j(k)], \end{aligned} \tag{9}$$

in consensus protocol. Where ε represents the interaction strength between DGs.

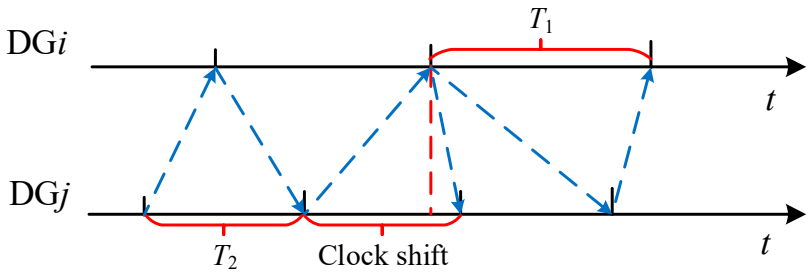

Figure 2. Schematic diagram of asynchronous communication.

On account of the dependency of the consensus algorithm on information synchronization, the system would ultimately converge to a consensus equilibrium deviated from the accurate value as

$$\Delta cx = (u' - u_2)\Delta z, \tag{10}$$

or even come to be unstable [26]. Where u_1, u_2 represents the left eigenvector corresponding to the eigenvalue 1 of the matrix A_s (listed in the Appendix A) and the Laplacian matrix, respectively;

$$u' = \left[\sum u_1(nk+1), \sum u_1(nk+2), \ldots \sum u_1(nk+n)\right]^T \text{and } \Delta z = [\Delta z_1,\ \Delta z_2,\ \ldots,\ \Delta z_n]^T \tag{11}$$

Essentially, the conventional consensus protocols assist in the achievement of system cooperation based on disagreement estimation and elimination between local and neighboring states and are valid only when the sampling intervals are restricted to be the same.

3. Fast Convergence Algorithm

3.1. Cooperative Control Using Fast Convergence Algorithm

Recalling the control objectives discussed in Section 2, the implementation of system cooperation requires both consistent incremental costs and average voltage restoration. If the unweighted average of incremental costs are defined as $\overline{\eta}$, i.e., $\overline{\eta} = \sum_{i=1}^{n} \eta_i / n$, then the objective of identical incremental costs can be equivalently converted to achieving the equilibrium where the incremental cost of each DG is equal to the average value $\overline{\eta}$.

On this basis, in view of the challenges of asynchronous sampling and time delays in the distributed consensus control, the fast convergence algorithm [27] is utilized in secondary control. In the algorithm, the dynamic state y_i and the weight w_i are designated as the inputs, where w_i is set to 1 for each DG in the unweighted average estimation required by cooperative control; two intermediate variables $\widetilde{s}_i$, $\widetilde{x}_i$ denoting the sum of the scales and scaled states, respectively, are introduced to assist the calculation of the estimated average value $\hat{x}_i$, which comes to be the output, and two new variables $s_{i\to j}$, $x_{i\to j}$ are defined to be the scale and scaled average state estimation transmitted from the ith node to the jth node and will be initialized to $s_{i\to j}(0) = \omega_i$ and $x_{i\to j}(0) = y_i$, respectively. The iterative execution of the algorithm is presented in Algorithm 1.

Algorithm 1: Fast convergence algorithm

Input: y_i and w_i are designated as the inputs.
Output: The average estimation of y_i denoted as $\widetilde{x}_i$ is the output.
For the kth iteration of the ith DG, execute the following calculation:

$$\widetilde{s}_i(k+1) = w_i + \sum_{j\in N_i} s_{j\to i}(k), \tag{12a}$$

$$\widetilde{x}_i(k+1) = w_i y_i + \sum_{j\in N_i} s_{j\to i}(k) x_{j\to i}(k), \tag{12b}$$

$$\hat{x}_i(k+1) = \frac{\widetilde{x}_i(k+1)}{\widetilde{s}_i(k+1)} \tag{12c}$$

Then, for each neighbor of the ith DG, calculate the following information:

$$s_{i\to j}(k+1) = \widetilde{s}_i(k+1) - s_{j\to i}(k), \tag{12d}$$

$$x_{i\to j}(k+1) = \frac{\widetilde{x}_i(k+1) - s_{j\to i}(k) x_{j\to i}(k)}{\widetilde{s}_i(k+1) - s_{j\to i}(k)} \tag{12e}$$

and transmit them to the jth DG.

For the ith node, the detailed execution of average incremental cost or voltage estimation conducted per iteration is illustrated as follows, which consists of three steps:

Step 1: Calculate the auxiliary variables $\widetilde{s}_i$, $\widetilde{x}_i$ based on information sampled locally and received from neighbors, which represents all information known by the ith node.

Step 2: Estimate the average value of the incremental cost η_i or voltage V_i using the auxiliary variables derived in Step 1.

Step 3: For any $j \in N_i$, calculate the information to be transmitted from the ith DG to the jth DG in preparation for the next iteration, which includes all information known by the ith DG except for those acquired from the jth DG.

As can be deduced from the above steps, in the first iteration of each DGi, average estimation is conducted based on the limited knowledge of the neighboring states and the form of the proposed algorithm is consistent with the consensus algorithm, whereas information of DGs that are one more hop away from DGi will be accessible in each of the following iterations; thus, accurate average estimation can be implemented with states of all DGs acquired within finite iterations. Subsequently, the average incremental cost or voltage estimated by each DG will converge to the accurate unweighted average value gradually, that is:

$$\hat{\eta}_i = \frac{\eta_i}{n}, \hat{V}_i = \frac{V_i}{n} \tag{13}$$

Accordingly, the optimal current sharing controller can be designed as:

$$u_{\eta i}(k) = k_{i1} T_i [\hat{\eta}_i(k) - \eta_i(k)] \tag{14}$$

While as for the voltage regulation control, the dynamic consensus problem is involved and the controller can be established based on the deviation between the average and nominal value of output voltage; hence, the integrated control input can be ultimately formulated as:

$$u_i(k+1) - u_i(k) = u_{\eta i}(k) + k_{i2} T_i [V_{ref} - \hat{V}_i(k)] \quad (15)$$

The concrete implementation structure of the cooperative control is depicted in Figure 3.

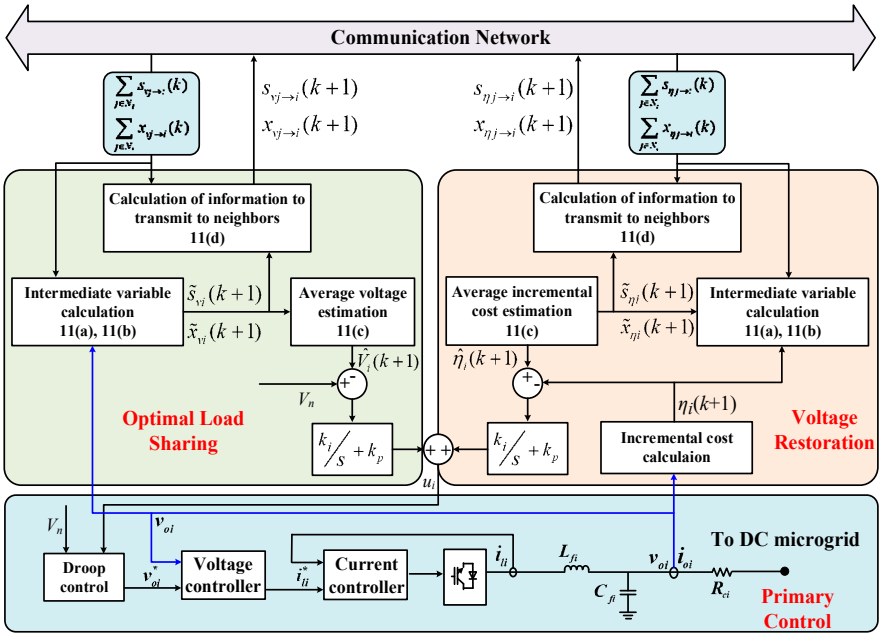

Figure 3. Implementation structure of distributed control adopting fast convergence algorithm.

3.2. Remarks of Algorithm

Convergence: Benefiting from the efficient information transmission, the fast convergence rate can be achieved using the proposed algorithm. Provided the ith node is reachable to the jth node through $(d_{ij}-1)$ intermediate nodes in the communication topology and the farthest distance between two nodes is $d = \max(d_{ij})$, then it can be concluded that global information can be broadcast to each node after d iterations, implying the system will converge asymptotically after at least d iterations. Compared with the limited knowledge of neighboring information by each node in the consensus algorithm, the information interaction efficiency is greatly improved. Additionally, information derived from one node will not be sent back to it again from any neighbors, indicating the avoidance of repetitive data transmission, which further contributes to the fast convergence performance of the proposed algorithm.

Asynchronous implementation: Another attractive feature of the algorithm is its adaptation to asynchronous sampling situations. In this case, initial information y_i, w_i of each node i will be transmitted to its neighbors at its local control instant, with the time index of the ith DG denoted as k_i incremented. Then, local average estimation and calculation of $s_{i\to j}(k_i)$, $x_{i\to j}(k_i)$ will be conducted once information from all the neighbors of the ith DG has been received. During the process, the correctness of data is guaranteed. In contrast to the strict requirement for the accurate measurement of disagreement between local and neighboring states from the same timeslot in consensus algorithm, the convergence of the proposed algorithm relies on the accessibility of global information, which can be implemented ultimately through the aforementioned asynchronous execution, only taking a longer period.

4. Stability Analysis

In this section, the sufficient stability condition for the proposed control scheme is derived based on the large-signal dynamic model.

The large-signal dynamic model for the system is first established, which consists of an inverter, network and loads.

Considering that the voltage and current loop possesses much faster dynamics compared with the power loop, the inverter can be modeled as follows, while ignoring the dynamics of the double-loop:

$$V_i(k) = V_{refi} - \gamma_i i_i(k) + u_i(k), \tag{16}$$

$$u_i(k+1) - u_i(k) = k_{i1} T_i[\hat{\eta}_i(k) - \eta_i(k)] + k_{i2} T_i[V_{ref} - \hat{V}_i(k)], \tag{17}$$

where the estimated average states can be obtained based on the control scheme proposed in Section 3. A:

$$\widetilde{S}_v(k+1) = \mathbf{1} + AS_v(k), \tag{18}$$

$$\widetilde{X}_v(k+1) = V(k+1) + A\cdot[\sum_{k=1}^{P} I_k\cdot(X_v(k)\cdot S_v(k)^T)\cdot I_k]\cdot E, \tag{19}$$

$$S_v(k+1) = B\widetilde{S}_v(k+1) - CX_v(k), \tag{20}$$

$$X_v(k+1) = [\sum_{k=1}^{P} I_k\cdot(X_v(k+1)\cdot E^T)\cdot I_k]^{-1}\cdot[B\cdot X_v(k+1) - C\cdot(\sum_{k=1}^{P} I_k\cdot(X_v(k)\cdot S_v(k)^T)\cdot I_k)\cdot E], \tag{21}$$

$$\hat{V}(k+1) = [\sum_{k=1}^{P} I_k\cdot(\widetilde{S}_v(k+1)\cdot E^T)\cdot I_k]^{-1}\cdot\widetilde{X}_v(k+1), \tag{22}$$

$$V(k+1) = V(k) + \frac{R}{\alpha}[\eta(k) - \eta(k+1)] + k_1 T[\overline{\eta}(k) - \eta(k)] + k_2 T[V_{ref} - \hat{V}(k)], \tag{23}$$

$$\widetilde{S}_\eta(k+1) = \mathbf{1} + AS_\eta(k), \tag{24}$$

$$\widetilde{X}_\eta(k+1) = \eta(k+1) + A\cdot[\sum_{k=1}^{P} I_k\cdot(X_\eta(k)\cdot S_\eta(k)^T)\cdot I_k]\cdot E, \tag{25}$$

$$S_\eta(k+1) = B\widetilde{S}_\eta(k+1) - CS_\eta(k), \tag{26}$$

$$X_\eta(k+1) = [\sum_{k=1}^{P} I_k\cdot(X_\eta(k+1)\cdot E^T)\cdot I_k]^{-1}\cdot[B\cdot X_\eta(k+1) - C\cdot(\sum_{k=1}^{P} I_k\cdot(X_\eta(k)\cdot S_\eta(k)^T)\cdot I_k)\cdot E], \tag{27}$$

$$\hat{\eta}(k+1) = [\sum_{k=1}^{P} I_k\cdot(\widetilde{S}_\eta(k+1)\cdot E^T)\cdot I_k]^{-1}\cdot\widetilde{X}_\eta(k+1), \tag{28}$$

where $\widetilde{S}$, $\widetilde{X}$ are vectors composed of the intermediate state variables of all DGs, while S, X are vectors regarding the scale and scaled average value, with the subscript η and v corresponding to the load sharing control and voltage restoration control, respectively; $\hat{\eta} = [\hat{\eta}_1, \hat{\eta}_2, \cdots \hat{\eta}_n]^T$, $\hat{V} = [\hat{V}_1, \hat{V}_2, \cdots \hat{V}_n]^T$, $\eta = [\eta_1, \eta_2, \ldots, \eta_n]^T$, $V = [V_1, V_2, \ldots, V_n]^T$ are the estimated and actual average voltage and incremental cost vectors and A, B, C, E, I_k are matrices listed in the Appendix A; $\mathbf{1} = [1,1, \ldots, 1]^T$.

Accordingly, η can be calculated by:

$$\eta_i(k+1) = \alpha i_i(k+1) + \beta \tag{29}$$

Supposing n DGs are connected through the network displayed in Figure 4, the output current can be then expressed as:

$$i = Y(V - V_b), \tag{30}$$

where $i = [i_1, i_2, \ldots, i_n]^T$, $V = [V_1, V_2, \ldots, V_n]^T$, and $V_b = [V_{b1}, V_{b2}, \ldots, V_{bn}]^T$ denotes the bus voltage; and $Y = \mathrm{diag}(y_i)$, where y_i is the output admittance of the ith DG.

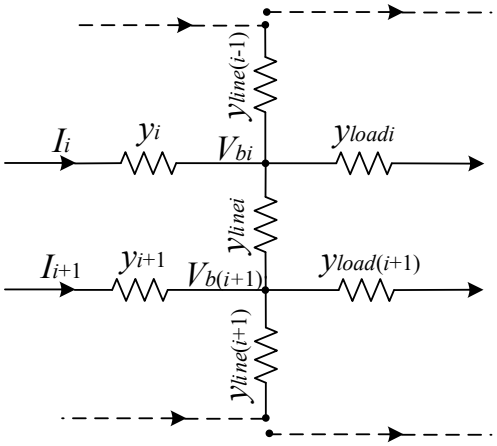

Figure 4. Network configuration.

Based on the node voltage equation, it yields

$$y_{si}V_{bi} = y_{line(i-1)}V_{b(i-1)} + y_{linei}V_{b(i+1)} + y_iV_i, \tag{31}$$

where $y_{si} = y_{linei} + y_{line(i-1)} + y_i + y_{loadi}$ with y_{linei} and y_{loadi} representing the line and load admittances, respectively.

Therefore, the relationship between output current and voltage can be established as:

$$i = Y'V, \tag{32}$$

where Y' is the admittance matrix as shown in the Appendix A.

Combing (2) and (16)~(32), the large-signal dynamic model of overall system can be arranged in a compact form

$$z(k+1) = f(z(k)), \tag{33}$$

where $z = [\widetilde{S}_v, \widetilde{X}_v, \hat{V}, V, \widetilde{S}_\eta, \widetilde{X}_\eta, \hat{\eta}, \eta]^T$.

Then, we will give the sufficient convergence condition for the system in (33).

Theorem 1. *The system will convergence asymptotically as long as the following inequality holds*:

$$J'(z_0)\cdot J'(z_0)^T < 0 \tag{34}$$

where $J'(z_0) = (J(z_0) - I)/T$ with I representing the identity matrix and J representing the Jacobi matrix of $f(z)$, which can be derived as

$$J = \frac{\partial f(z)}{\partial z^T} = \begin{bmatrix} J_1 & J_2 & J_3 & J_4 & J_5 & J_6 & J_7 & J_8 \end{bmatrix}^T \tag{35}$$

with $J_1 = [B\cdot A\text{-}C\ 0\ 0\ 0\ 0\ 0\ 0\ 0]$; $J_2 = [J_{21}\ J_{22}\ 0\ 0\ 0\ 0\ 0\ 0] + H_1J_4$; $J_3 = [J_{31}\ J_{32}\ 0\ 0\ 0\ 0\ 0\ 0] + H_2J_4$; $J_4 = [0\ 0\ \text{-}k_2T\cdot I\ I\text{-}\omega_c\gamma Y'\ 0\ 0\ k_1T\cdot I\ H_3\text{-}k_1T\cdot I]$; $J_5 = [0\ 0\ 0\ B\cdot A\text{-}C\ 0\ 0\ 0\ 0]$; $J_6 = [0\ 0\ 0\ 0\ J_{61}\ J_{62}\ 0\ 0] + H_4J_8$; $J_7 = [0\ 0\ 0\ 0\ J_{71}\ J_{72}\ 0\ 0] + H_5J_8$ and $J_8 = [0\ 0\ 0\ \text{-}\omega_cT\boldsymbol{\alpha}Y'\ 0\ 0\ 0\ (1\text{-}\omega_cT)I]$, where $\boldsymbol{\gamma} = diag(\gamma_i)$ and $\boldsymbol{\alpha} = diag(\alpha_i)$, J_{21}, J_{22}, J_{31}, J_{32}, J_{61}, J_{62}, J_{71}, J_{72}, H_1, H_2, H_3, H_4, H_5 are matrices given in the Appendix A.

Proof. First, (33) can be rewritten as:

$$\frac{z(k+1)-z(k)}{T} = \frac{f(z(k))-z(k)}{T} \tag{36}$$

Accordingly, its continuous counterpart can be derived as

$$\dot{z} = \frac{f(z)-z}{T} \tag{37}$$

Consider the Lyapunov function $V(z)$= $\dot{V}(z) = \dot{z}^T\dot{z}$ and the derivative of $V(z)$ can be expressed as

$$\dot{V}(z) = \left(\frac{\dot{f}(z)-\dot{z}}{T}\right)^T \cdot \dot{z} + \dot{z}^T \cdot \left(\frac{\dot{f}^T(z)-\dot{z}}{T}\right) \tag{38}$$

According to the derivation rule of complex functions, the following equation holds for the time derivative of $f(z)$:

$$\dot{f}(z) = \frac{\partial f(z)}{\partial z^T} \cdot \frac{\partial z}{\partial t} = J \cdot \dot{z} \tag{39}$$

Substituting (39) to (38), the derivative of $V(z)$ can be rearranged to the form as (40):

$$\dot{V}(z) = \left[\left(\frac{J-I}{T}\right)\cdot\dot{z}\right]^T \dot{z} + \dot{z}^T\left[\left(\frac{J-I}{T}\right)\cdot\dot{z}\right] = \dot{z}^T\left[J'^T \cdot J'\right]\dot{z} \tag{40}$$

Given the condition that J' is negative definite, it can be deduced from (40) that $\dot{V}(z)$ is negative definite, leading to the conclusion that the system will come to be stable asymptotically. □

5. Simulation Results

Case studies are carried out to verify the effectiveness of the proposed secondary control using the test MG as shown in Figure 5, where five DGs with identical rating and three loads are connected to the voltage bus. The system and control parameters are listed in Table 1.

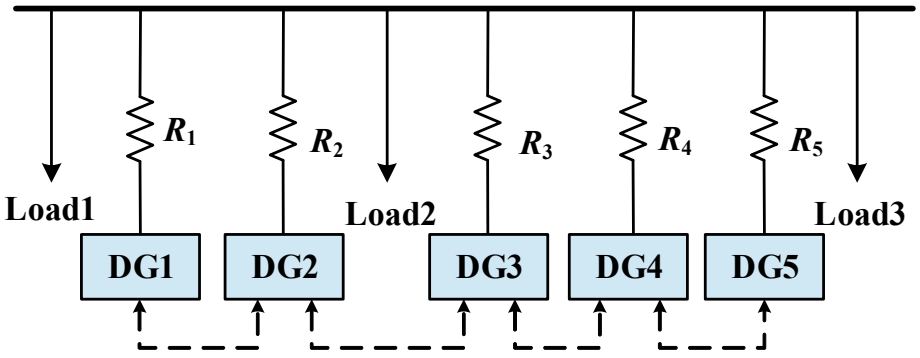

Figure 5. Configuration of the test MG.

Table 1. Network and control parameters.

Parameter	Value	Parameter	Value
MG voltage	800 V	Generation Cost Coefficient	
DG power ratings		$\alpha_1/\alpha_2/\alpha_3/\alpha_4/\alpha_5$	0.08/0.08/0.08/0.06/0.06
P_1, P_2, P_3, P_4, P_5	30 kW	$\beta_1/\beta_2/\beta_3/\beta_4/\beta_5$	1.42/1.42/1.42/0.96/0.96
Voltage droop coefficient		Connection and load parameter	
$\gamma_1, \gamma_2, \gamma_3, \gamma_4, \gamma_5$	0.8 V/A	$R_1/R_2/R_3$	0.15 Ω/0.30 Ω/0.40 Ω
Control parameters		R_4/R_5	0.25 Ω/ 0.20 Ω
$k_{i1}/k_{i2}/k_{i3}$	6/10/3	$r_{load1}/r_{load2}/r_{load3}$	25 Ω/20 Ω/30 Ω

5.1. Conventional Performance

The performance of the proposed scheme is compared with the consensus protocol under a unified sampling period T = 0.01 s. The MG is initially controlled by droop control, and the cooperative secondary control is activated at t = 3 s, with an additional load (10 kW) attached to the bus at t = 7 s. The corresponding active powers, output voltages and incremental costs are shown in Figure 6b. For comparison with the distributed consensus control, the MG is operated with the same controller gains and communication topology, with the results shown in Figure 6a. As shown in both Figure 6a,b, the inappropriate power sharing and voltage deviation emerge initially due to droop characteristics. After the activation of secondary control, expected load sharing and voltage restoration are achieved and can be maintained in spite of the increase or decrease in the load. Nevertheless, the transient process in Figure 6a takes a much longer time than Figure 6b. With a further enlargement of the sampling period to 0.05 s, the system installed with consensus-based cooperative controller fails to remain stable, due to the growing oscillation in the curves in Figure 7a. By contrast, the active powers and voltages in Figure 7b show a slight fluctuation and comes to be stable rapidly, which indicates that the proposed algorithm has a superior robustness to sampling periods.

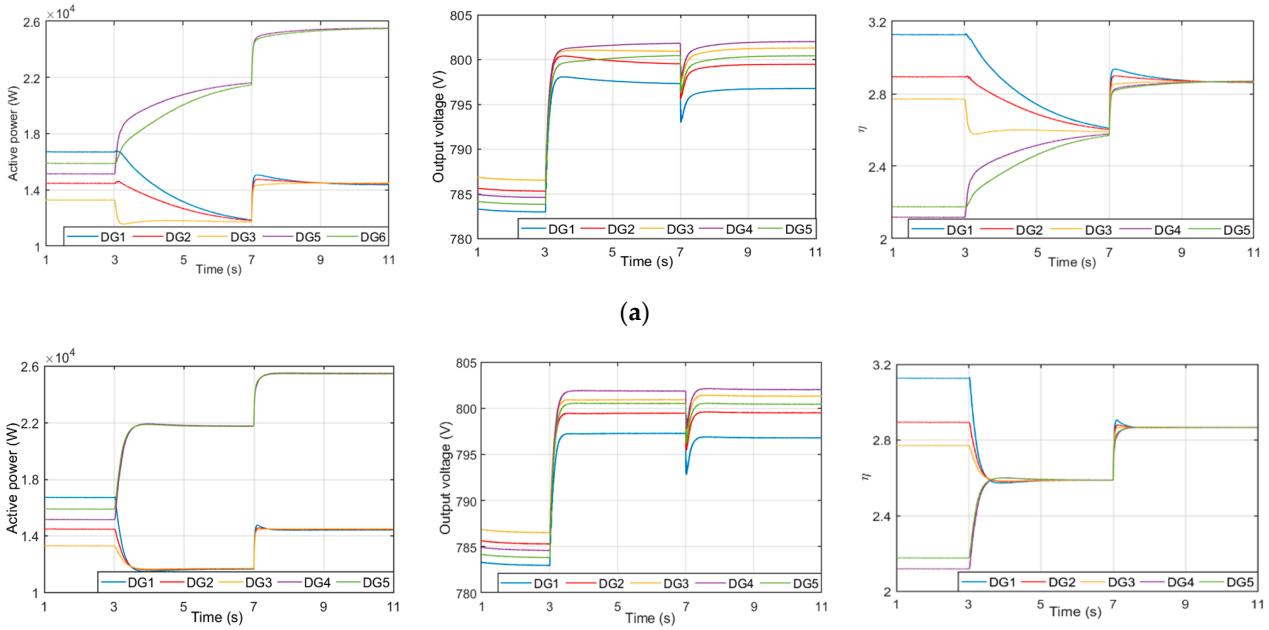

Figure 6. Simulation results of active powers, output voltages and incremental costs in synchronous communication case. (**a**) Consensus algorithm. (**b**) Fast convergence algorithm.

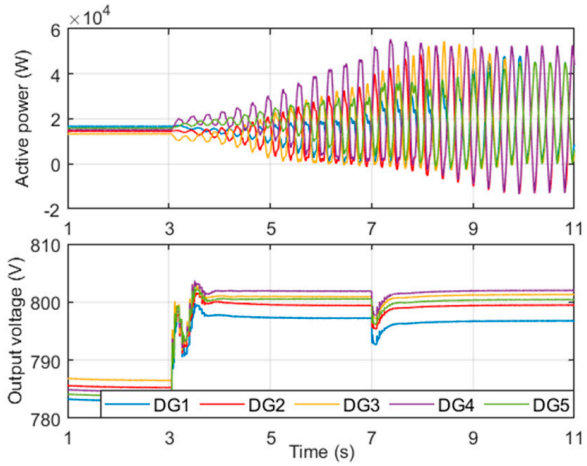

(**a**)

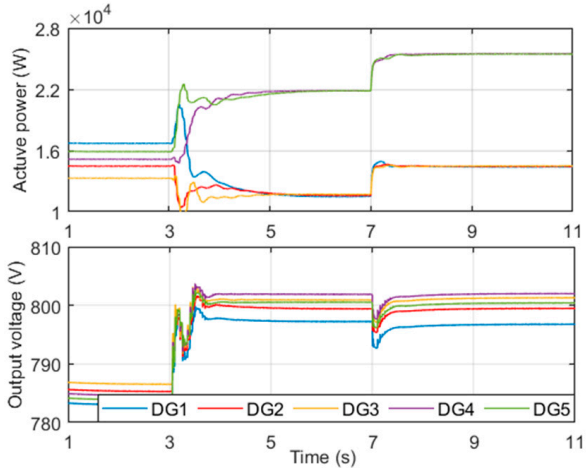

(**b**)

Figure 7. Simulation results of active powers and output voltages with sampling interval as 0.05 s using different algorithms. (**a**) Consensus algorithm. (**b**) Fast convergence algorithm.

5.2. Arbitrary Sampling

The asynchronous consensus concern that is inherent in distributed control is investigated in this case. Due to the absence of a centralized clock, uncertainties inevitably occur and are assumed to be within $\pm 10\% T_i$ on the basis of the individual sampling periods $T_1 = 0.05$ s, $T_2 = 0.01$ s, $T_3 = 0.02$ s, $T_4 = 0.06$ s, $T_5 = 0.07$ s, with associated arbitrary sampling intervals shown in Figure 8 [28]. Simulation results in this case are displayed in Figure 9, from which it can be observed that the system under the consensus protocol is obviously unstable and the system with the proposed control remains stable due to decaying oscillations. Therefore, the proposed control scheme demonstrates excellent robustness to arbitrary sampling compared with the conventional consensus algorithm because of its inherent asynchronous implementation, elaborated in Section 3. On the other hand, considering the maximum allowable sampling interval $T = 0.05$ s in the synchronous case, the communication cost can be reduced drastically by 28.57% from the perspective of DG5.

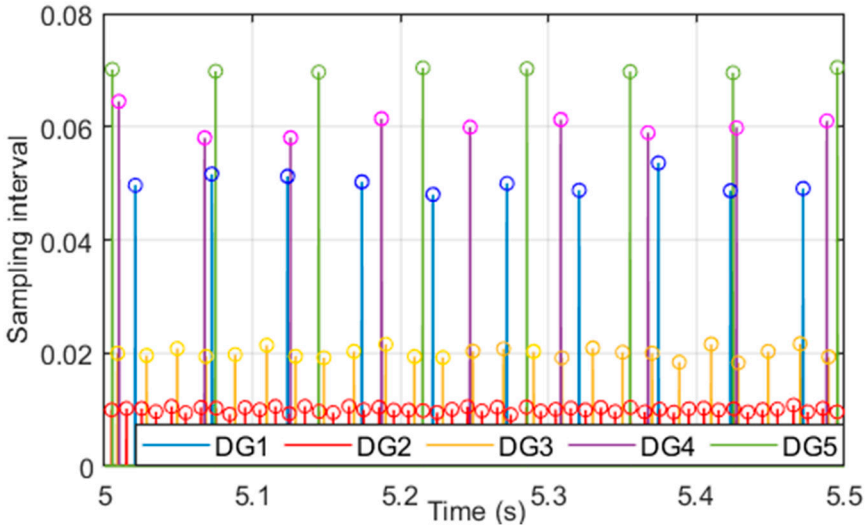

Figure 8. Arbitrary sampling intervals assuming uncertainties within $\pm 10\% T_i$ on the basis of individual sampling periods $T_1 = 0.05$ s, $T_2 = 0.01$ s, $T_3 = 0.02$ s, $T_4 = 0.06$ s, $T_5 = 0.07$ s.

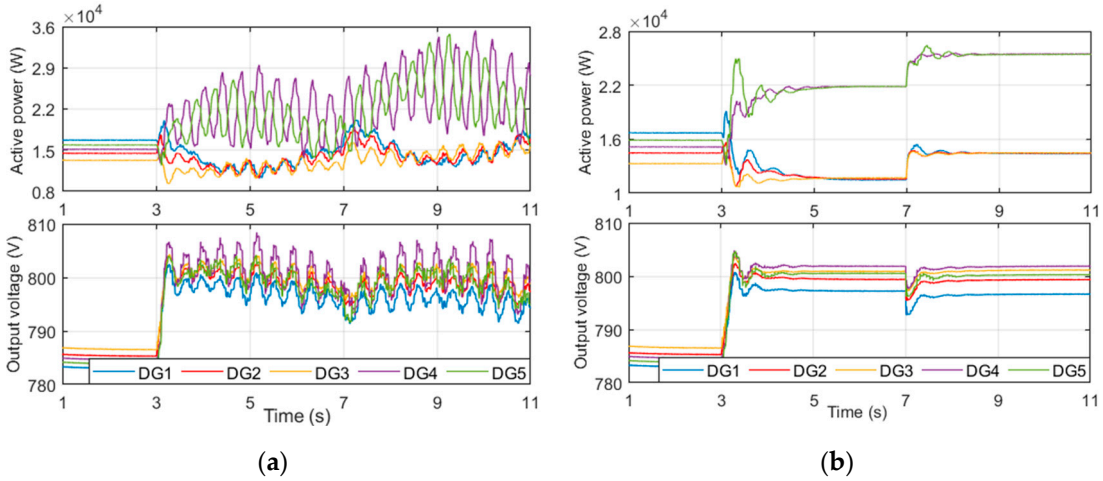

Figure 9. Simulation results under arbitrary sampling as shown in Figure 8. (**a**) Consensus algorithm. (**b**) Fast convergence algorithm.

5.3. Discussion

As can be deduced from Figure 6, economic load sharing and voltage restoration can be achieved simultaneously with a faster convergence rate using the proposed control strategy, indicating the proposed scheme is effective and has a loose constraint on communication topology for better convergence performance. Moreover, based on comparison between Figure 7a,b, it can obviously be seen that the proposed control strategy enjoys enhanced stability in the case of large sampling intervals, which would contribute to lower controlling cost. Ultimately, the better robustness to arbitrary sampling of the proposed scheme is demonstrated by Figure 9. In conclusion, the secondary control method proposed in this paper shows great superiority compared with conventional consensus-based secondary control, and can be well integrated with the existing hierarchical control strategies [29–31].

6. Conclusions

In this paper, a novel algorithm which addresses the average consensus problem with higher transmission efficiency is introduced and applied in cooperative control of microgrids. Employing the approach of the Lyapunov function, the sufficient stability

condition for the algorithm is derived. Comparative study has revealed the superiority of the algorithm over the consensus algorithm in terms of convergence rate and its adaptability to the arbitrary sampling case.

Author Contributions: Software, Y.H.; writing—original draft preparation, Y.H. writing—review and editing, J.X.; J.X.; project administration, F.F. All authors have read and agreed to the published version of the manuscript.

Funding: This research was funded by Science and Technology Project of State Grid Zhejiang Electric Power Co., Ltd., Grant 5211DS16002F.

Institutional Review Board Statement: Not applicable.

Informed Consent Statement: Not applicable.

Data Availability Statement: This study did not report any data.

Conflicts of Interest: The authors declare no conflict of interest.

Nomenclature

V_i	output reference voltage
V_{refi}	nominal voltage
γ_i	droop coefficient
i_i	output current
i_{oi}	instantaneous current
α_i, β_i, ρ_i	related coefficients of the cost function
η_i	incremental cost
$\overline{V}_i$	average voltage estimated by the ith DG
u_i	secondary control input
T_i	local sampling interval of the ith DG
k_{i1}, k_{i2}, k_{i3}	integral gains
i_{Li}	the ith load current
i_D	the total load demand
w_i	weight in the average calculation
y_i	dynamic state
$\overline{\eta}$	weighted average incremental cost
$s_{i\to j}$	scale
$x_{i\to j}$	scaled average state estimation
$\widetilde{s}_i$	sum of the scales
$\widetilde{x}_i$	sum of the scaled states
$\hat{x}_i$	estimated average value

Abbreviations

DG	Distributed generations
MG	Microgrids
MGCC	Microgrid centralized controller

Appendix A

Suppose that p_{ij} is the total number of possible sampling instant offsets during information transmission from the jth DG to ith DG.

$$A_s = \begin{bmatrix} & A_1 \\ I_{n\cdot r_{\max}\times n\cdot r_{\max}} & [0]_{n\cdot r_{\max}\times n\cdot h} \end{bmatrix}_{n\cdot(h+r_{\max})\times n\cdot(h+r_{\max})}$$

where

$$A_1 = \begin{bmatrix} {C'}_{n\times n\cdot(h+r_{\max})} \\ \vdots \\ {C'}_{n\times n\cdot(h+r_{\max})} \end{bmatrix}_{n\cdot h\times n\cdot(h+r_{\max})},$$

I is the identity matrix and

$$C' = \begin{bmatrix} [0]_{n\times n\cdot(h-1)} & H_{n\times n} & W_{n\times n\cdot r_{\max}} \end{bmatrix}_{n\times n\cdot(h+r_{\max})}$$

with

$$H_{n\times n} = \begin{bmatrix} 1-\varepsilon T_1 & \frac{\varepsilon T_1}{p_{12}} & \cdots & \frac{\varepsilon T_1}{p_{1n}} \\ \frac{\varepsilon T_2}{p_{21}} & 1-\varepsilon T_2 & \cdots & \frac{\varepsilon T_2}{p_{2n}} \\ \vdots & \vdots & \ddots & \vdots \\ \frac{\varepsilon T_n}{p_{n1}} & \frac{\varepsilon T_n}{p_{n2}} & \cdots & 1-\varepsilon T_n \end{bmatrix}_{n\times n};$$

$$W(i, n\cdot(m-1)+j) = \begin{cases} \frac{\varepsilon T_i}{p_{ij}} & if \exists k \in [1, p_{ij}], r_{ij,k} = m \\ 0 & otherwise \end{cases}$$

The vectors of state variables can be expressed as:

$$\widetilde{s}_v = [\widetilde{s}_{v1}, \widetilde{s}_{v2}, \cdots, \widetilde{s}_{vn}]^T, \widetilde{x}_v = [\widetilde{x}_{v1}, \widetilde{x}_{v2}, \cdots, \widetilde{x}_{vn}]^T, \widetilde{s}_\eta = [\widetilde{s}_{\eta 1}, \widetilde{s}_{\eta 2}, \cdots, \widetilde{s}_{\eta n}]^T, \widetilde{x}_\eta = [\widetilde{x}_{\eta 1}, \widetilde{x}_{\eta 2}, \cdots, \widetilde{x}_{\eta n}]^T,$$
$$\hat{\eta} = [\hat{\eta}_1, \hat{\eta}_2, \cdots, \hat{\eta}_n]^T, \hat{V} = [\hat{V}_1, \hat{V}_2, \cdots, \hat{V}_n]^T, \eta = [\eta_1, \eta_2, \ldots, \eta_n]^T, V = [V_1, V_2, \ldots, V_n]^T,$$
$$S_v = \left[s_{v1\to q1(1)}, \ldots, s_{v1\to q1(p1)}, s_{v2\to q2(1)}, \ldots, s_{v2\to q2(p2)}, \ldots, s_{vn\to qn(1)}, \ldots, s_{vn\to qn(pn)}\right]^T,$$
$$x_v = \left[x_{v1\to q1(1)}, \ldots, x_{v1\to q1(p1)}, x_{v2\to q2(1)}, \ldots, x_{v2\to q2(p2)}, \ldots, x_{vn\to qn(1)}, \ldots, x_{vn\to qn(pn)}\right]^T,$$
$$s_\eta = \left[s_{\eta_1\to q1(1)}, \ldots, s_{\eta_1\to q1(p1)}, s_{\eta_2\to q2(1)}, \ldots, s_{\eta_2\to q2(p2)}, \ldots, s_{\eta_n\to qn(1)}, \ldots, s_{\eta_n\to qn(pn)}\right]^T,$$
$$x_\eta = \left[x_{\eta_1\to q1(1)}, \ldots, x_{\eta_1\to q1(p1)}, x_{\eta_2\to q2(1)}, \ldots, x_{\eta_2\to q2(p2)}, \ldots, x_{\eta_n\to qn(1)}, \ldots, x_{\eta_n\to qn(pn)}\right]^T.$$

Define the set of neighbors of the ith DG as $N_i = \{q_i(1), q_i(2), \ldots, q_i(p_i)\}$ and the degree of the ith DG can be expressed as $p_i = \sum_j a_{ij}$ The coefficient matrices of the algorithm can be expressed as:

$$A(i,j) = \begin{cases} 1 & if \quad j = \sum_{k=1}^{m-1} p_k + l, where \quad q_m(l) = i \\ 0 & otherwise \end{cases}; \quad B(i,j) = \begin{cases} 1 & if \quad \sum_{k=1}^{j-1} p_k < i \le \sum_{k=1}^{j} p_k \\ 0 & otherwise \end{cases}$$

$$C(i,j) = \begin{cases} 1 & if \quad i = \sum_{k=1}^{m1-1} p_k + l_1, j = \sum_{k=1}^{m2-1} p_k + l_2, \\ & where \quad m2 = q_{m1}(l_1), m1 = q_{m2}(l_2) \\ 0 & otherwise \end{cases}; \quad I_k(i,j) = \begin{cases} 1 & if \quad i = j = k \\ 0 & otherwise \end{cases}$$

The matrices in Jacobi matrix can be derived as:

$$H_1(i,j) = \begin{cases} \frac{1}{1+\sum_{ij} {s'}_v} & if \quad \sum_{k=1}^{j-1} p_k < i \le \sum_{k=1}^{j} p_k \\ 0 & otherwise \end{cases}$$

$$\sum_{ij} {s'}_v = \sum_{h=1}^{P} \sigma_{ih} s_v(h); \ \sum_{ij} s_v \cdot {x_v}' = \sum_{h=1}^{P} \sigma_{ih} s_v(h) x_v(h); \ \sigma_{ih} = \begin{cases} 1 & \begin{array}{l} if \quad i = \sum_{k=1}^{m1-1} p_k + l_1 \quad where \quad q_{m1}(l_1) = m2; \\ h = \sum_{k=1}^{\delta-1} p_k + l_2, q_\delta(l_2) = m1 \quad and \quad \delta \ne m2 \end{array} \\ 0 & otherwise \end{cases}$$

$$J_{31}(i,j)=\begin{cases}\frac{x_v(j)(1+\sum_i s_v)-(V(i)+\sum_i s_v\cdot x_v)}{(1+\sum_i s_v)^2} & if \quad j=\sum_{k=1}^{m-1}p_k+l \\ & where \quad q_m(l)=i \\ 0 & otherwise\end{cases}$$

$$J_{32}(i,j)=\begin{cases}\frac{s_v(j)}{1+\sum_i s_v} & if \quad j=\sum_{k=1}^{m-1}p_k+l \quad where \quad q_m(l)=i \\ 0 & otherwise\end{cases};\ H_2(i,j)=\begin{cases}\frac{1}{1+\sum_i s_v} & if \quad j=i \\ 0 & otherwise\end{cases};$$

$$\sum_i s_v=\sum_{h=1}^{P}\mu_{ih}s_v(h);\ \sum_i s_v\cdot x_v=\sum_{h=1}^{P}\mu_{ih}s_v(h)x_v(h);\ \mu_{ih}=\begin{cases}1 & if \quad h=\sum_{k=1}^{\delta-1}p_k+l \quad and \quad q_\delta(l)=i \\ 0 & otherwise\end{cases}$$

$$H_3=\begin{bmatrix}\frac{\gamma_1}{\alpha_1}\omega_c T & 0 & \cdots & 0 \\ 0 & \frac{\gamma_2}{\alpha_2}\omega_c T & \ddots & \vdots \\ \vdots & \ddots & \ddots & 0 \\ 0 & \cdots & 0 & \frac{\gamma_n}{\alpha_n}\omega_c T\end{bmatrix};\ H_4(i,j)=\begin{cases}\frac{1}{1+\sum_{ij}s'_\eta} & if \quad \sum_{k=1}^{j-1}p_k<i\le\sum_{k=1}^{j}p_k \\ 0 & otherwise\end{cases}$$

$$\sum_{ij}s'_\eta=\sum_{h=1}^{P}\sigma_{ih}s_\eta(h);\ \sum_{ij}s_\eta\cdot x_\eta{}'=\sum_{h=1}^{P}\sigma_{ih}s_\eta(h)x_\eta(h);\ J_{71}(i,j)=\begin{cases}\frac{x_\eta(j)(1+\sum_i s_\eta)-(\eta(i)+\sum_i s_\eta\cdot x_\eta)}{(1+\sum_i s_\eta)^2} & if \quad j=\sum_{k=1}^{m-1}p_k+l \\ & where \quad q_m(l)=i \\ 0 & otherwise\end{cases}$$

$$H_5(i,j)=\begin{cases}\frac{1}{1+\sum_i s_\eta} & if \quad j=i \\ 0 & otherwise\end{cases};\ \sum_i s_\eta=\sum_{h=1}^{P}\mu_{ih}s_\eta(h);\ \sum_i s_\eta\cdot x_\eta=\sum_{h=1}^{P}\mu_{ih}s_\eta(h)x_\eta(h)$$

$$J_{72}(i,j)=\begin{cases}\frac{s_\eta(j)}{1+\sum_i s_\eta} & if \quad j=\sum_{k=1}^{m-1}p_k+l \quad where \quad q_m(l)=i \\ 0 & otherwise\end{cases}$$

$$J_{21}(i,j)=\begin{cases}\frac{x_v(j)(1+\sum_{ij}s'_v)-(V(m1)+\sum_{ij}s_v\cdot x'_v)}{(1+\sum_{ij}s'_v)^2} & if \quad i=\sum_{k=1}^{m1-1}p_k+l_1, j=\sum_{k=1}^{m3-1}p_k+l_3, where \quad m2=q_{m1}(l_1), m1=q_{m3}(l_3), m3\in N_{m1}\backslash\{m2\} \\ 0 & otherwise\end{cases}$$

$$J_{22}(i,j)=\begin{cases}\frac{s_v(j)}{1+\sum_{ij}s'_v} & if \quad i=\sum_{k=1}^{m1-1}p_k+l_1, j=\sum_{k=1}^{m3-1}p_k+l_3, where \quad m2=q_{m1}(l_1), m1=q_{m3}(l_3), m3\in N_{m1}\backslash\{m2\} \\ 0 & otherwise\end{cases}$$

$$J_{61}(i,j)=\begin{cases}\frac{x(j)(1+\sum_{ij}s'_\eta)-(\eta(m1)+\sum_{ij}s_\eta\cdot x'_\eta)}{(1+\sum_{ij}s'_\eta)^2} & if \quad i=\sum_{k=1}^{m1-1}p_k+l_1, j=\sum_{k=1}^{m3-1}p_k+l_3, where \quad m2=q_{m1}(l_1), m1=q_{m3}(l_3), m3\in N_{m1}\backslash\{m2\} \\ 0 & otherwise\end{cases}$$

$$J_{62}(i,j)=\begin{cases}\frac{s_\eta(j)}{1+\sum_{ij}s'_\eta} & if \quad i=\sum_{k=1}^{m1-1}p_k+l_1, j=\sum_{k=1}^{m3-1}p_k+l_3, where \quad m2=q_{m1}(l_1), m1=q_{m3}(l_3), m3\in N_{m1}\backslash\{m2\} \\ 0 & otherwise\end{cases}$$

References

1. Schiffer, J.; Seel, T.; Raisch, J.; Sezi, T. Voltage stability and reactive power sharing in inverter-based microgrids with consensus-based distributed voltage control. *IEEE Trans. Control. Syst. Technol* **2016**, *24*, 96–109. [CrossRef]
2. Sadabadi, M.S.; Shafiee, Q.; Karimi, A. Plug-and-play voltage stabilization in inverter-interfaced microgrids via a robust control strategy. *IEEE Trans. Control. Syst. Technol.* **2017**, *25*, 781–791. [CrossRef]
3. Liu, S.; Wang, X.; Liu, P.X. Impact of communication delays on secondary frequency control in an islanded microgrid. *IEEE Trans. Ind. Electron.* **2015**, *62*, 2021–2031. [CrossRef]
4. Qian, T.; Liu, Y.; Zhang, W.; Tang, W.; Shahidehpour, M. Event-triggered updating method in centralized and distributed secondary controls for islanded microgrid restoration. *IEEE Trans. Smart Grid* **2020**, *11*, 1387–1395. [CrossRef]
5. Colet-Subirachs, A.; Ruiz-Alvarez, A.; Gomis-Bellmunt, O.; Alvarez-Cuevas-Figuerola, F.; Sudria-Andreu, A. Centralized and distributed active and reactive power control of a utility connected microgrid using IEC61850. *IEEE Syst. J.* **2012**, *6*, 58–67. [CrossRef]
6. Dou, C.; Yue, D.; Guerrero, J.M.; Xie, X.; Hu, S. Multiagent system-based distributed coordinated control for radial DC microgrid considering transmission time delays. *IEEE Trans. Smart Grid* **2017**, *8*, 2370–2381. [CrossRef]
7. Nasirian, V.; Moayedi, S.; Davoudi, A.; Lewis, F.L. Distributed cooperative control of DC microgrids. *IEEE Trans. Power Electron.* **2015**, *30*, 2288–2303. [CrossRef]
8. Dong, M.; Li, L.; Nie, Y.; Song, D.; Yang, J. Stability analysis of a novel distributed secondary control considering communication delay in DC microgrids. *IEEE Trans. Smart Grid* **2019**, *10*, 6690–6700. [CrossRef]
9. Abdelaziz, M.M.A.; Shaaban, M.F.; Farag, H.E.; El-Saadany, E.F. A multistage centralized control scheme for islanded microgrids with PEVs. *IEEE Trans. Sustain. Energy* **2014**, *5*, 927–937. [CrossRef]
10. Huang, P.; Liu, P.; Xiao, W.; Moursi, M.S.E. A novel droop-based average voltage sharing control strategy for DC microgrids. *IEEE Trans. Smart Grid* **2015**, *6*, 1096–1106. [CrossRef]
11. Wu, X.; Xu, Y.; He, J.; Wang, X.; Vasquez, J.C.; Guerrero, J.M. Pinning-based hierarchical and distributed cooperative control for AC microgrid clusters. *IEEE Trans. Power Electron.* **2020**, *35*, 9865–9885. [CrossRef]
12. Kumar, R.; Pathak, M.K. Distributed droop control of dc microgrid for improved voltage regulation and current sharing. *Iet Renew. Power Gen.* **2020**, *14*, 2499–2506. [CrossRef]
13. Guo, F.; Wang, L.; Wen, C.; Zhang, D.; Xu, Q. Distributed voltage restoration and current sharing control in islanded DC microgrid systems without continuous communication. *IEEE Trans. Ind. Electron.* **2020**, *67*, 3043–3053. [CrossRef]
14. Baranwal, M.; Askarian, A.; Salapaka, S.; Salapaka, M. A distributed architecture for robust and optimal control of DC microgrids. *IEEE Trans. Ind. Electron.* **2019**, *66*, 3082–3092. [CrossRef]
15. Zhang, R.; Hredzak, B. Distributed finite-time multiagent control for DC microgrids with time delays. *IEEE Trans. Smart Grid* **2019**, *10*, 2692–2701. [CrossRef]
16. Lee, G.; Ko, B.; Cho, J.; Kim, R. A distributed control method based on a voltage sensitivity matrix in DC microgrids with low-speed communication. *IEEE Trans. Smart Grid* **2019**, *10*, 3809–3817. [CrossRef]
17. Zhan, J.; Li, X. Asynchronous consensus of multiple double-integrator agents with arbitrary sampling intervals and communication delays. *IEEE Trans. Circuits Syst Ireg. Pap.* **2015**, *62*, 2301–2311. [CrossRef]
18. Fu, J.; Wen, G.; Yu, W.; Huang, T.; Cao, J. Exponential consensus of multiagent systems with Lipschitz nonlinearities using sampled-data information. *IEEE Trans. Circuits Syst. Ireg. Pap.* **2018**, *65*, 4363–4375. [CrossRef]
19. Mattioni, M. On multiconsensus of multi-agent systems under aperiodic and asynchronous sampling. *IEEE Contr. Syst. Lett.* **2020**, *4*, 839–844.
20. Li, Z.; Shahidehpour, M. Small-signal modeling and stability analysis of hybrid AC/DC microgrids. *IEEE Trans. Smart Grid* **2019**, *10*, 2080–2095. [CrossRef]
21. Lou, G.; Gu, W.; Xu, Y.; Jin, W.; Du, X. Stability robustness for secondary voltage control in autonomous microgrids with consideration of communication delays. *IEEE Trans. Power Syst.* **2018**, *33*, 4164–4178. [CrossRef]
22. Coelho, E.A.; Wu, D.; Guerrero, J.M.; Vasquez, J.C.; Dragičević, T.; Stefanović, C.; Popovski, P. Small-signal analysis of the microgrid secondary control considering a communication time delay. *IEEE Trans. Ind. Electron.* **2016**, *63*, 6257–6269. [CrossRef]
23. Duan, J.; Chow, M. Robust consensus-based distributed energy management for microgrids with packet losses tolerance. *IEEE Trans. Smart Grid* **2020**, *11*, 281–290. [CrossRef]
24. Atay, F.M. Consensus in networks under transmission delays and the normalized Laplacian. *IFAC Proc. Vol.* **2010**, *43*, 277–282. [CrossRef]
25. Lai, J.; Lu, X.; Yu, X.; Monti, A.; Zhou, H. Distributed voltage regulation for cyber-physical microgrids with coupling delays and slow switching topologies. *IEEE Trans. Syst. Man Cybern. Syst.* **2020**, *50*, 100–110. [CrossRef]
26. Du, Y.; Tu, H.; Yu, H.; Lukic, S. Accurate consensus-based distributed averaging with variable time delay in support of distributed secondary control algorithms. *IEEE Trans. Smart Grid* **2020**, *11*, 2918–2928. [CrossRef]
27. Xie, K.; Cai, Q.; Zhang, Z.; Fu, M. Distributed algorithms for average consensus of input data with fast convergence. *IEEE Trans. Syst. Man Cybern. Syst.* **2021**, *51*, 2653–2664. [CrossRef]
28. Guo, G.; Ding, L.; Han, Q.L. A distributed event-triggered transmission strategy for sampled-data consensus of multi-agent systems. *Automatica* **2014**, *50*, 1489–1496. [CrossRef]

29. Baghaee, H.R.; Mirsalim, M.; Gharehpetian, G.B. Real-time verification of new controller to improve small/large-signal stability and fault ride-through capability of multi-DER microgrids. *IET Gener. Transm. Distrib.* **2016**, *10*, 3068–3084. [CrossRef]
30. Baghaee, H.R.; Mirsalim, M.; Gharehpetian, G.B.; Talebi, H.A. Unbalanced harmonic power sharing and voltage compensation of microgrids using radial basis function neural network-based harmonic power-flow calculations for distributed and decentralised control structures. *IET Gener. Transm. Distrib.* **2018**, *12*, 1518–1530. [CrossRef]
31. Baghaee, H.R.; Mirsalim, M.; Gharehpetian, G.B. Power calculation using RBF neural networks to improve power sharing of hierarchical control scheme in multi-DER microgrids. *IEEE J. Emerg. Sel. Top. Power Electron.* **2016**, *4*, 1217–1225. [CrossRef]